

## Topology-driven nonlinear switching in Möbius discrete arrays

Francisco J. Muñoz,<sup>1,2</sup> Sergei K. Turitsyn,<sup>3</sup> Yuri S. Kivshar,<sup>4</sup> and Mario I. Molina<sup>1,5</sup>

<sup>1</sup>*Departamento de Física, Facultad de Ciencias, Universidad de Chile, Santiago, Chile*

<sup>2</sup>*Center for the Development of Nanoscience and Nanotechnology (CEDENNA), Santiago, Chile*

<sup>3</sup>*Research School of Physics and Engineering, Aston University, Birmingham B4 7ET, United Kingdom*

<sup>4</sup>*Nonlinear Physics Centre, Australian National University, Canberra ACT 2601, Australia*

<sup>5</sup>*MSI-Nucleus on Advanced Optics, Facultad de Ciencias, Universidad de Chile, Santiago, Chile*

(Received 14 November 2016; published 24 March 2017)

We examine the switching dynamics of discrete solitons propagating along two coupled discrete arrays which are twisted to form a Möbius strip. We analyze the potential of the topological switches by comparing the differences between the Möbius strip and untwisted discrete arrays. We employ the Ablowitz-Ladik (AL) model and reveal a nontrivial Berry phase associated with the monopole spectra in parameter space. We study the dynamical evolution of the AL soliton launched into one of the chains and observe its switching behavior. While in the untwisted discrete case, the soliton splits in nearly identical portions as the interchain coupling is increased, in the Möbius case and for weak coupling, we observe a well-defined “switching time” where the soliton switches completely from one chain to the other.

DOI: [10.1103/PhysRevA.95.033833](https://doi.org/10.1103/PhysRevA.95.033833)

### I. INTRODUCTION

Topological insulators represent a novel class of materials with topologically protected order [1], and they are promising for potential applications. The ever-increasing interest of the physics community was patently demonstrated with the awarding of the 2016 Nobel Prize in Physics to three researchers who made the seminal contributions in this field. Recently, the general concepts of topological insulators and topological phase order became very attractive in optics, and different types of electromagnetic topological states have been suggested theoretically and realized experimentally for microwave and optical systems [2]. More importantly, photonic systems have been used to simulate conventional topological systems and to explore topological phases, mainly in the waveguide geometry [3] and bi-anisotropic metamaterials [4]. By employing the bulk-edge correspondence, one may explore different topological phases by probing edge states or edge topological invariants in optics [5].

Apart from the multiple efforts to emulate topological insulators and their properties, in optics there are many examples of relatively simple models to realize different types of photonic topological states. One of the examples, a dimer chain (known also as the Su-Schrieffer-Heeger model) [6], was implemented for optical edge modes in a binary waveguide array [7]. Analogous systems have been recently proposed to demonstrate one-dimensional topological edge states based on zigzag chains of nanoparticles [8].

Twisted Möbius strips are known for their unusual topological properties of being surfaces with only one side. Recently, such strips were generated optically by tightly focusing the light beam emerging from a liquid crystal  $q$  plate [9], revealing the appearance of Möbius polarization structures of light, driven by this unusual topology. An important difference between the Möbius strip and other topological systems (e.g., the SSH model) is that the topology is determined by the boundary conditions rather than from the Hamiltonian.

In this article we uncover fascinating properties of the Möbius geometry by studying the effect of topology in coupled

discrete arrays, including the switching of discrete solitons. We reveal that the nontrivial Berry phase associated with the parameter space of the twisted pair of coupled discrete arrays stipulates the unusual switching dynamics of discrete solitons, with a sharp difference between the Möbius and untwisted chains. We believe that such topological modes may be important for topological optical switches and complex light beam engineering in photonic networks, and may bring additional knowledge about the role of topology in optics.

### II. SPECTRAL PROPERTIES OF COUPLED DISCRETE ARRAYS

We consider the propagation of a discrete soliton [10] along a quasi-one-dimensional (ribbon) lattice [11], with the topology of a Möbius strip [Fig. 1(a)]. We are interested in the effect of this nontrivial topology on the switching behavior of the soliton. The results will be compared with those of a usual ribbon with untwisted boundary conditions [Fig. 1(b)]. We will use the simplest ribbon consisting of two coupled chains, chain  $A$  and chain  $B$ .

*Untwisted boundary conditions.* Let us consider a discrete ribbon formed by two coupled chains ( $A$  and  $B$ ). Assuming periodic boundary conditions (untwisted), the Hamiltonian of each chain is

$$H_{\delta} = -t \sum_{i=1}^N c_{\delta,i}^{\dagger} c_{\delta,i+1} + \text{H.c.}, \quad (1)$$

where  $\delta = \{A, B\}$  denote the different chains,  $t$  is the nearest neighbor hopping, and  $c_{\delta,N+1} = c_{\delta,1}$ .

When the two chains are coupled, with one  $A$  site on top of a  $B$  site, we will end with  $N$  coupled dimers, each composed of an  $A, B$  pair. If the  $A$ - $B$  hopping is  $t'$ , the interchain Hamiltonian reads

$$H_{AB} = -t' \sum_{i=1}^N c_{A,i}^{\dagger} c_{B,i} + \text{H.c.} \quad (2)$$

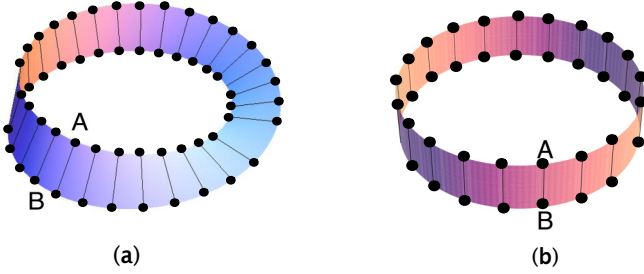


FIG. 1. Geometry of the two ribbons considered in this work: (a) Möbius and (b) untwisted.

Even though it is straightforward to solve this Hamiltonian by the Fourier transform, we will take a detour which will make it easier to solve the Möbius strip later.

The eigenvalue equation ( $H_{\text{untwisted}}\Psi = E\Psi$ ) for each site is reduced to the form

$$tC_{n-1} + tC_{n+1} + t'\sigma_x C_n = EC_n, \quad (3)$$

where  $\sigma_x$  is one of the Pauli matrices.

That suggests a solution  $C_n = e^{ikn} \begin{pmatrix} a \\ b \end{pmatrix}$  which results in a simple equation for the eigenvalues

$$\begin{pmatrix} 2t \cos(k) - E & t' \\ t' & 2t \cos(k) - E \end{pmatrix} \begin{pmatrix} a \\ b \end{pmatrix} = 0, \quad (4)$$

with solutions

$$E_{\pm} = 2t \cos(k) \pm t', \quad C_n = \frac{e^{ikn}}{\sqrt{2}} \begin{pmatrix} 1 \\ \pm 1 \end{pmatrix}. \quad (5)$$

Now we apply the periodic boundary condition to obtain the allowed values of  $k$ . From the condition  $C_{N+1} = C_1$ , we obtain

$$e^{ikN} = 1 \Rightarrow k = \frac{2m\pi}{N}, \quad m = 0, 1, 2, \dots, N-1. \quad (6)$$

*Möbius boundary conditions.* Now we consider the discrete Möbius strip. To impose Möbius boundary conditions to the ribbon composed of the two chains  $A$  and  $B$ , we need to close the loop by attaching the  $A$  site from an end of the ribbon to the  $B$  site of the other end of the ribbon, and vice versa. This leads to the same Hamiltonian [Eqs. (1) and (2)] as in the untwisted case for all the sites *except* at the twisted boundary. Thus, the only difference between  $H_{\text{untwisted}}$  and  $H_{\text{Möbius}}$  is at the boundaries, where  $H_{\text{Möbius}}(1, N) = t\sigma_x$ , reflecting that an  $A$  site has a  $B$  neighbor.

We write the eigenvalue equations in an explicit form:

$$tC_{n-1} + tC_{n+1} + t'\sigma_x C_n = EC_n, \quad 1 < n < N, \quad (7)$$

$$t\sigma_x C_N + tC_2 + t'\sigma_x C_1 = EC_1, \quad (8)$$

$$tC_{N-1} + t\sigma_x C_1 + t'\sigma_x C_N = EC_N. \quad (9)$$

The similarity between  $H_{\text{untwisted}}$  and  $H_{\text{Möbius}}$  is evident, and it should lead to a similar spectrum, if we take the limit of an infinitely long chain. Thus, by disregarding the borders, the eigenvalue equations (7) are the same as in (3). These considerations suggest we use the same solutions of the untwisted case (5), before imposing the boundary conditions.

While Eq. (5) satisfies Eq. (7), we still need to solve the eigenvalue equation at the boundaries, namely Eqs. (8) and (9). Let us take the solution for the untwisted case:

$$E_+ = t \cos(k) + t', \quad C_+ = \frac{e^{ikn}}{\sqrt{2}} \begin{pmatrix} 1 \\ 1 \end{pmatrix}, \quad (10)$$

with  $k$  not yet defined, and apply it to both boundary equations, obtaining

$$te^{ik(N-1)} \begin{pmatrix} 1 \\ 1 \end{pmatrix} + te^{ik} \begin{pmatrix} 1 \\ 1 \end{pmatrix} + t' \begin{pmatrix} 1 \\ 1 \end{pmatrix} = [2t \cos(k) + t'] \begin{pmatrix} 1 \\ 1 \end{pmatrix}, \quad (11)$$

$$te^{-ik} \begin{pmatrix} 1 \\ 1 \end{pmatrix} + te^{ik(N+1)} \begin{pmatrix} 1 \\ 1 \end{pmatrix} + t' \begin{pmatrix} 1 \\ 1 \end{pmatrix} = [2t \cos(k) + t'] \begin{pmatrix} 1 \\ 1 \end{pmatrix}, \quad (12)$$

both equations (left and right borders) are redundant and satisfied if  $k = 2\pi m/N$ . That is the same result found in the untwisted case.

The remaining eigenvalue and eigenvector (of the untwisted case) are

$$E_- = t \cos(k) - t', \quad C_- = \frac{e^{ikn}}{\sqrt{2}} \begin{pmatrix} 1 \\ -1 \end{pmatrix}. \quad (13)$$

After substituting it into the boundary equations, we obtain

$$\begin{aligned} te^{ik(N-1)} \begin{pmatrix} -1 \\ 1 \end{pmatrix} + te^{ik} \begin{pmatrix} 1 \\ -1 \end{pmatrix} + t' \begin{pmatrix} -1 \\ 1 \end{pmatrix} \\ = [2t \cos(k) - t'] \begin{pmatrix} 1 \\ -1 \end{pmatrix}, \end{aligned} \quad (14)$$

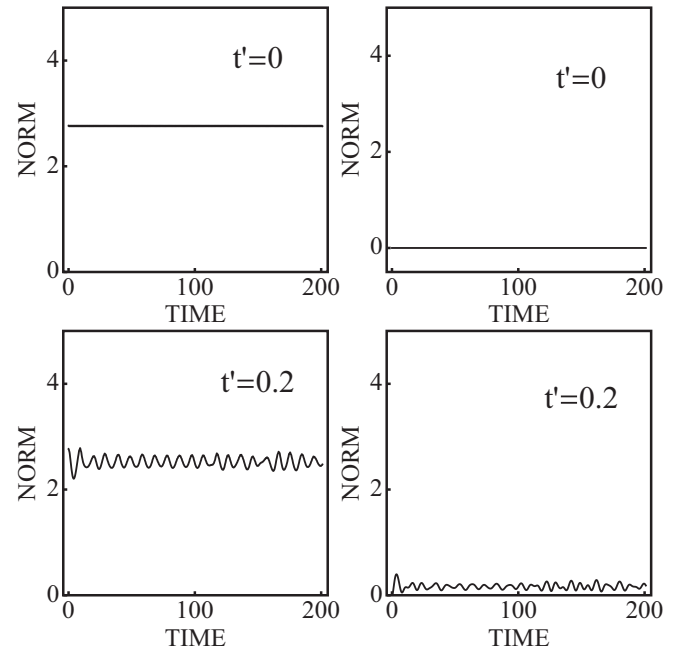


FIG. 2. Untwisted case. Soliton norm of the AL soliton on chain  $A$  (left column) and on chain  $B$  (right column), for two values of interchain coupling ( $\alpha = 1, \beta = 0.5, N = 103$ ).

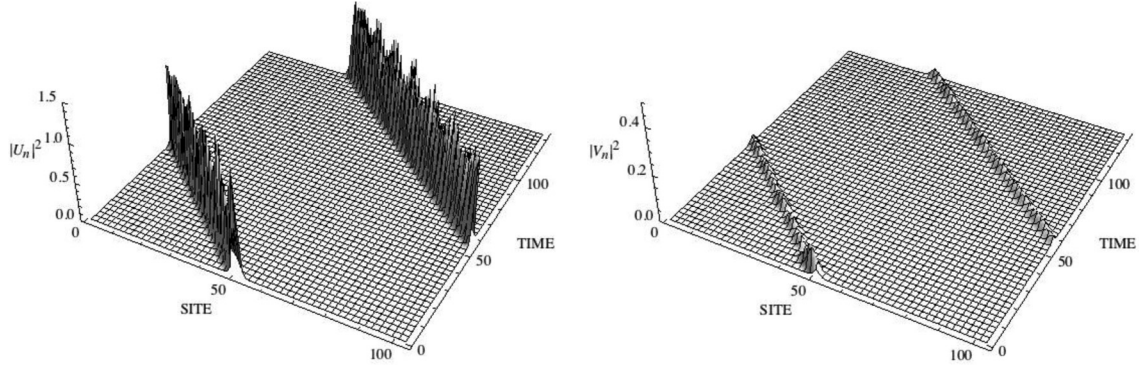


FIG. 3. Untwisted case. Time evolution of  $u_n(z)$  (left) and  $v_n(z)$  (right) for an initial AL soliton for a normal untwisted strip, and for a small transverse coupling value  $t' = 0.2$  ( $\alpha = 1, \beta = 0.5, N = 103$ ).

$$\begin{aligned} & t e^{-ik} \begin{pmatrix} 1 \\ -1 \end{pmatrix} + t e^{ik(N+1)} \begin{pmatrix} -1 \\ 1 \end{pmatrix} + t' \begin{pmatrix} -1 \\ 1 \end{pmatrix} \\ & = [2t \cos(k) - t'] \begin{pmatrix} 1 \\ -1 \end{pmatrix}. \end{aligned} \quad (15)$$

In order to satisfy these equations, it is needed

$$e^{ikN} = -1 \Rightarrow k = \frac{m\pi}{N}, \quad m = 1, 3, \dots, 2N - 1. \quad (16)$$

This solution, evidently, has a period of  $2N$ , twice the number of sites.

Finally, we calculate the geometrical (Berry) phase [12] associated with both states of the Möbius strip. This phase is defined as

$$\gamma_{\pm} = -i \sum_{n=1}^N C_{\pm}(n) \frac{\partial}{\partial n} C_{\pm}(n) = -i \int_0^N dn C_{\pm}(n) \frac{\partial}{\partial n} C_{\pm}(n), \quad (17)$$

assuming that the chain is long enough to have a continuum range of  $n$ . Since a phase is defined only up to  $2\pi$ , we obtain the values  $\gamma_- = \pi$  and  $\gamma_+ = 0$ .

The value  $\gamma_- = \pi$  reflects the fact that it is impossible to use a single gauge everywhere [13]. For instance, let us think that the  $A$  sites are positive and the  $B$  sites are negative. After traveling through the whole chain, the sites  $A$  and  $B$  need to change their sign, i.e., another gauge. In contrast, the case of  $C_+$  has a trivial Berry's phase, indicating that a single phase (or gauge) is enough to cover all the sites, since after

walking through the whole chain, and exchanging  $A$  and  $B$  sites, the phase is the same. Also, and contrary to the situation in topological insulators, which also have a Berry phase of  $\pi$ , in our system the  $\pi$  geometrical phase comes from the boundary conditions, not from the Hamiltonian.

A nontrivial Berry's phase indicates the existence of a monopole similar to a magnetic monopole but living in the parameter space [14]. This extra phase is similar to the Aharonov-Bohm effect due a magnetic field, but with an important difference: enclosing a Berry's magnetic monopole does not break the time-reversal symmetry (this is why it is exactly  $\pi$ ).

### III. DYNAMICS OF DISCRETE SOLITONS

Let us now consider a discrete soliton propagating along the coupled chains. We are interested in the way the soliton switches between the two chains, when in the presence of untwisted or Möbius boundary conditions. To work with a *bona fide* integrable discrete soliton we use the Ablowitz-Ladik (AL) equation [15] expanded for the case of two coupled chains:

$$\begin{aligned} i \frac{du_n(z)}{dz} + [t + \chi |u_n(z)|^2](u_{n+1} + u_{n-1}) + t' v_n(z) &= 0, \\ i \frac{dv_n(z)}{dz} + [t + \chi |v_n(z)|^2](v_{n+1} + v_{n-1}) + t' u_n(z) &= 0, \end{aligned} \quad (18)$$

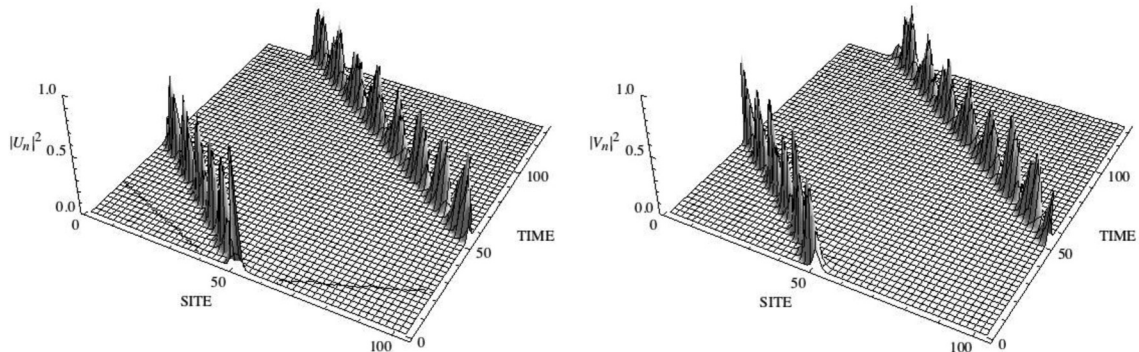


FIG. 4. Untwisted case. Time evolution of  $u_n(z)$  (left) and  $v_n(z)$  (right) for an initial AL soliton for a normal untwisted strip, and for a transverse coupling value  $t' = 0.5$  ( $\alpha = 1, \beta = 0.5, N = 103$ ).

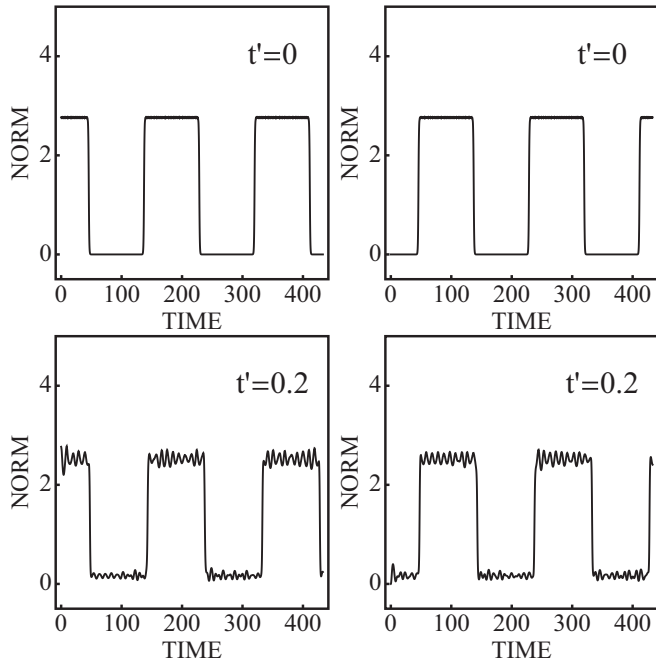


FIG. 5. Möbius case. Soliton norm of the AL soliton in chains A (left) and B (right) as a function of time, for interchain coupling  $t' = 0$  and  $t' = 0.2$  ( $\alpha = 1, \beta = 0.5, N = 433$ ).

where  $u_n$  and  $v_n$  are the excitation amplitudes on chains A and B, respectively,  $\chi$  is the nonlinearity parameter, and we have taken a simple linear coupling between both chains, parametrized by  $t'$ . For a single chain, the AL equation admits a closed-form solution in the form of a discrete soliton (the AL soliton):

$$u_n(z) = \sinh(\alpha) \operatorname{sech}(\alpha n + vz) \exp[-i(\beta n + \omega z)] \quad (19)$$

written in dimensionless units, where  $\alpha$  and  $\beta$  are parameters that determine the velocity and frequency of the soliton:

$$v = 2 \sinh(\alpha) \sin(\beta), \quad (20)$$

$$\omega = -2 \cosh(\alpha) \cos(\beta). \quad (21)$$

Equation (20) provides a natural time scale for an AL soliton propagating along a chain with untwisted. This time

corresponds to the time it takes the soliton to traverse the length of the chain and come back to the initial position. For a chain of  $N$  sites, this characteristic time is

$$T = \frac{N}{2 \sinh(\alpha) \sin(\beta)}. \quad (22)$$

The idea now is to examine the propagation of an AL soliton in a discrete Möbius strip and in the presence of coupling between the two chains. We seek to find how the nontrivial topology of the Möbius ribbon influences the switching behavior of the AL soliton. The results will be compared to the ones obtained for the simple untwisted topology.

To quantify the degree of localization of the excitation on any of the two chains, we will resort to the soliton norm (SN), defined as

$$N^{(u)} = \sum_n |u_n|^2, \quad N^{(v)} = \sum_n |v_n|^2, \quad (23)$$

which gives a measure of the fraction of the soliton present on a given chain. The total norm  $N \equiv N^{(u)} + N^{(v)}$  is a dynamical constant, as can be obtained from Eq. (18).

For the periodic boundary conditions case, we have

$$u_1 = u_{N+1}, \quad v_1 = v_{N+1}, \quad (24)$$

and solve Eqs. (18) to trace the evolution of  $u_n, v_n$ , using as an initial condition the AL soliton profile placed on one of the chains,  $u_n(0) = \sinh(\alpha) \operatorname{sech}(\alpha n) \exp(-\beta n)$  and  $v_n(0) = 0$ . Figure 2 shows the time evolution of the soliton norms on chains A and B, for a couple of interchain coupling values. Figures 3 and 4 show the time evolution of  $u(z)$  and  $v(z)$ , for two coupling values. From these figures we observe that in the presence of interchain coupling, the soliton stays mainly on the initial chain (chain A), while the small portion that is transferred to chain B gives rise to a another, smaller soliton that propagates with the same speed as the “main” soliton. That is, the initial soliton has been split into two solitons by the presence of the interchain coupling. As the interchain coupling increases so does the size of soliton B. When all couplings (interchain and intrachain) have the same value, the initial AL soliton gets split into two, nearly identical AL-type solitons. In this respect the coupled chains system acts as a coherent coupler [16].

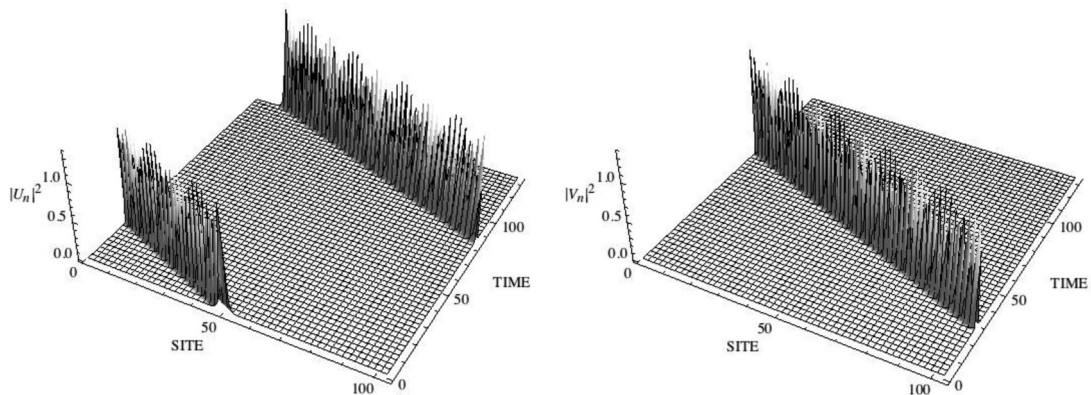


FIG. 6. Möbius case. Time evolution of  $u_n(z)$  (left) and  $v_n(z)$  (right) for an initial AL soliton on a Möbius strip, in the absence of transversal coupling  $t' = 0$  ( $\alpha = 1, \beta = 0.5, N = 103$ ).

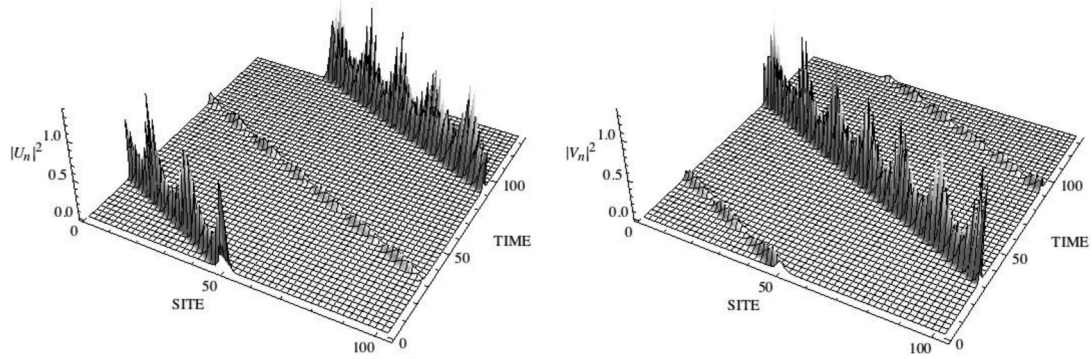


FIG. 7. Möbius case. Time evolution of  $u_n(z)$  (left) and  $v_n(z)$  (right) for an initial AL soliton on a Möbius strip, for transversal coupling  $t' = 0.26$  ( $\alpha = 1, \beta = 0.5, N = 103$ ).

As stated earlier, to obtain the Möbius case, one has to impose a special boundary condition by coupling the  $A$  site from one end of the strip to the  $B$  site to the other end of the ribbon, and vice versa. More explicitly, the boundary terms in Eq. (18) read

$$\begin{aligned} i(du_1/dz) + (t + \chi|u_1|^2)(u_2 + v_N) + t'v_1 &= 0, \\ i(du_N/dz) + (t + \chi|u_N|^2)(u_{N-1} + v_1) + t'v_N &= 0, \\ i(dv_1/dz) + (t + \chi|v_1|^2)(v_2 + u_N) + t'u_1 &= 0, \\ i(dv_N/dz) + (t + \chi|v_N|^2)(v_{N-1} + u_1) + t'u_N &= 0. \end{aligned} \quad (25)$$

As we did for the untwisted case, we solve numerically Eqs. (18) and (25) for  $u_n$  and  $v_n$ , using as an initial condition the AL soliton placed on one of the chains. We focus on the switching behavior of the soliton as the interchain parameter  $t'$  is varied. Typical results are shown in Fig. 5, which shows the soliton norm on each chain, as a function of time. Contrary to the PR of the untwisted case, here we see an abrupt alternation between large and small soliton norm, indicating an abrupt switching.

In the absence of coupling, the AL soliton propagates on the initial chain for a while until, at time  $T$  it disappears from the initial chain and gets transferred completely to the other chain, where it will propagate for a time  $T$ , after which it will reappear on the initial chain, reaching the initial position at time  $2T$ . From the parameters used in Fig. 5, this recurrence time is  $2T = 182.8$ . We see that the presence of the Möbius

boundary conditions has produced a complete switching of the AL soliton (see Fig. 6). Now, for a nonzero interchain coupling, something interesting happens: As soon as the AL soliton on chain  $A$  gets switched to chain  $B$ , a small soliton is produced on chain  $A$  with the same speed as the AL soliton (Fig. 7). This intermediate soliton disappears from chain  $A$  as soon as the AL soliton gets switched back to chain  $A$  from chain  $B$ . Similarly, while the AL soliton is on chain  $A$ , the intermediate soliton propagates along chain  $B$ . The size of this intermediate soliton is proportional to the transverse coupling  $t'$ . When  $t'$  is large enough ( $\sim 0.5$ ), the size of the intermediate soliton is similar to the one of the AL soliton (Fig. 8). This case is dynamically indistinguishable from the untwisted case, and one only observes an AL soliton in chain  $A$  and another in chain  $B$  that propagate with the same speed on (effectively) untwisted chains. In addition to all of this, we also observe in all cases a high frequency oscillation of the soliton due to internal dynamics and interchain coupling, governed by the coupling parameter  $t'$ .

#### IV. CONCLUSIONS

We have examined the switching dynamics of an Ablowitz-Ladik (AL) soliton propagating along a twisted pair of discrete chains, mimicking a Möbius strip. We have found that the spectra of the system exhibits only one nontrivial geometric (Berry) phase,  $\gamma = \pi$ , similar to the Aharonov-Bohm effect, but without breaking of the time-reversal symmetry.

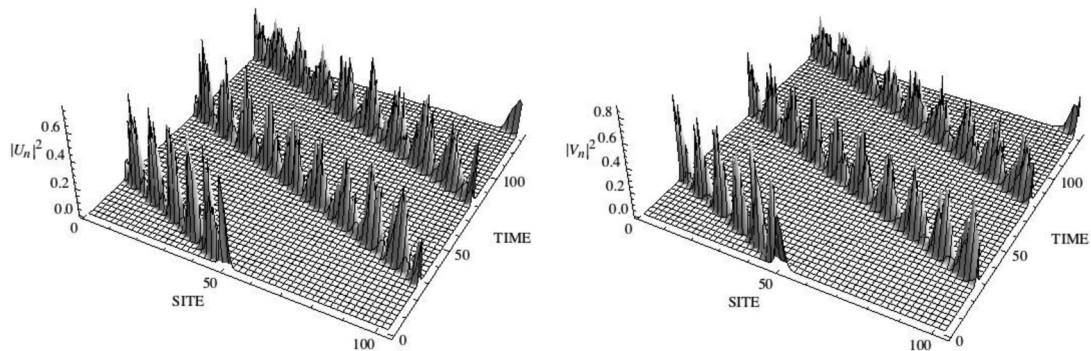


FIG. 8. Möbius case. Time evolution of  $u_n(z)$  (left) and  $v_n(z)$  (right) for an initial AL soliton on a Möbius strip, for transversal coupling  $t' = 0.5$  ( $\alpha = 1, \beta = 0.5, N = 103$ ).

In the absence of interchain coupling, we have observed switching of an AL soliton, with a well-defined period. In the presence of interchain coupling, this switching gets degraded by the presence of a single intermediate soliton, whose amplitude increases with the strength of the interchain coupling. At stronger interchain coupling, this leads to a dynamics that mimics the one with periodic boundary conditions.

## ACKNOWLEDGMENTS

This work was supported in part by Fondecyt Grants No. 1150806 and No. 1160177, Programa ICM Grant No. RC130001, the Center for the Development of Nanoscience and Nanotechnology CEDENNA FB0807, and the Australian Research Council, and the Liverhulme Trust through the Visiting Professorship Program.

- 
- [1] M. Z. Hasan and C. L. Kane, *Rev. Mod. Phys.* **82**, 3045 (2010); B. Bernevig and T. Hughes, *Topological Insulators and Topological Superconductors* (Princeton University Press, Princeton, NJ, 2013).
- [2] L. Lu, J. D. Joannopoulos, and M. Soljacic, *Nat. Photon.* **8**, 821 (2014).
- [3] M. C. Rechtsman, J. M. Zeuner, Y. Plotnik, Y. Lumer, D. Podolsky, F. Dreisow, S. Nolte, M. Segev, and A. Szameit, *Nature (London)* **496**, 196 (2013); M. Hafezi, S. Mittal, J. Fan, A. Migdall, and J. M. Taylor, *Nat. Photon.* **7**, 1001 (2013).
- [4] A. B. Khanikaev, S. Hossein Mousavi, W.-K. Tse, M. Kargarian, A. H. MacDonald, and G. Shvets, *Nat. Mater.* **12**, 233 (2013); A. P. Slobozhanyuk, A. B. Khanikaev, D. S. Filonov, D. A. Smirnova, A. E. Miroshnichenko, and Y. S. Kivshar, *Sci. Rep.* **6**, 22270 (2016); K. Lai, T. Ma, X. Bo, S. Anlagec, and G. Shvets, *ibid.* **6**, 28453 (2016).
- [5] S. Mittal, J. Fan, S. Faez, A. Migdall, J. M. Taylor, and M. Hafezi, *Phys. Rev. Lett.* **113**, 087403 (2014); A. V. Poshakinskiy, A. N. Poddubny, and M. Hafezi, *Phys. Rev. A* **91**, 043830 (2015).
- [6] J. K. Asboth, L. Oroszlany and A. Palyi, *A Short Course on Topological Insulators* (Springer, Berlin, 2016).
- [7] N. Malkova, I. Hromada, X. Wang, G. Bryant, and Z. Chen, *Opt. Lett.* **34**, 1633 (2009).
- [8] A. P. Slobozhanyuk, A. N. Poddubny, A. E. Miroshnichenko, P. A. Belov, and Y. S. Kivshar, *Phys. Rev. Lett.* **114**, 123901 (2015).
- [9] T. Bauer, P. Banzer, E. Karimi, S. Orlov, A. Rubano, L. Marrucci, E. Santamato, R. W. Boyd, and G. Leuchs, *Science* **347**, 964 (2015); T. Bauer, M. Neugebauer, G. Leuchs, and P. Banzer, *Phys. Rev. Lett.* **117**, 013601 (2016).
- [10] S. Trillo and W. Torruellas (eds.), *Spatial Solitons* (Springer, Berlin, 2001); J. W. Fleischer, M. Segev, N. K. Efremidis, and D. N. Christodoulides, *Nature (London)* **422**, 147 (2003); F. Lederer, G. I. Stegeman, D. N. Christodoulides, G. Assanto, M. Segev, and Y. Silberberg, *Phys. Rep.* **463**, 1 (2008); Yu. V. Bludov, D. A. Smirnova, Yu. S. Kivshar, N. M. R. Peres, and M. I. Vasilevskiy, *Phys. Rev. B* **91**, 045424 (2015).
- [11] M. I. Molina and Y. S. Kivshar, *Opt. Lett.* **35**, 2895 (2010).
- [12] M. V. Berry, *Proc. R. Soc. London Ser. A* **392**, 45 (1984); F. Wilczek and A. Shapere, *Geometric Phases in Physics* (World Scientific, Singapore, 1989); A. Bohm, A. Mostafazadeh, H. Koizumi, Q. Niu, and J. Zwanziger, *Foundations, Mathematical Concepts, and Applications in Molecular and Condensed Matter Physics* (Springer Science & Business Media, Berlin, 2013); N. Zhao, H. Dong, S. Yang, and C. P. Sun, *Phys. Rev. B* **79**, 125440 (2009); E. H. Martins Ferreira, M. C. Nemes, M. D. Sampaio, and H. A. Weidenmüller, *Phys. Lett. A* **333**, 146 (2004); W. Beugeling, A. Quelle, and C. Morais Smith, *Phys. Rev. B* **89**, 235112 (2014).
- [13] M. Fruchart and D. Carpentier, *C. R. Phys.* **14**, 779 (2013).
- [14] Z. L. Guo, Z. R. Gong, H. Dong, and C. P. Sun, *Phys. Rev. B* **80**, 195310 (2009).
- [15] M. J. Ablowitz and J. F. Ladik, *J. Math. Phys.* **17**, 1011 (1976); L. D. Faddeev and L. A. Takhtajan, *Hamiltonian Methods in the Theory of Solitons* (Springer, Berlin, 1987); M. J. Ablowitz and P. A. Clarkson, *Solitons, Nonlinear Evolution Equations and Inverse Scattering* (Cambridge University Press, New York, 1991); A. Bulow, D. Henning, and H. Gabriel, *Phys. Rev. E* **59**, 2380 (1999); M. I. Molina, *ibid.* **372**, 6388 (2008).
- [16] S. M. Jensen, *IEEE J. Quantum Electron.* **18**, 1580 (1982); W. D. Deering, M. I. Molina, and G. P. Tsironis, *Appl. Phys. Lett.* **62**, 2471 (1993).